Available online at www.sciencedirect.com
ScienceDirect
Inorganica Chimica Acta 360 (2007) 1072–1082
Inorganica Chimica Acta
www.elsevier.com/locate/ica

Photophysical, photochemical and electrochemical properties of a series of aromatic electron acceptors based on N-heterocycles

Roberto Ballardini [a], Alberto Credi [b,*], Maria Teresa Gandolfi [b,*], Carlo Giansante [b], Giancarlo Marconi [a], Serena Silvi [b], Margherita Venturi [b,*]

[a] *Istituto ISOF-CNR, via Gobetti 101, 40129 Bologna, Italy*
[b] *Dipartimento di Chimica "G. Ciamician", Università di Bologna, via Selmi 2, 40126 Bologna, Italy*

Received 28 July 2006; accepted 14 August 2006
Available online 30 August 2006

Dedicated to Professor Vincenzo Balzani on his 70th birthday.

Abstract

The electronic absorption and luminescence spectra, photoreactivity, and the electrochemical properties of a series of aromatic electron acceptors based on the 4,4′-bipyridinium, 1,2-bis(4-pyridinium)ethylene, and 2,7-diazapyrenium cations have been investigated. All these species exhibit distinctive absorption spectra and some of them show fluorescence and phosphorescence bands. The compounds based on the 1,2-bis(4-pyridinium)ethylene unit provide the interesting possibility of studying the *E*–*Z* photoisomerization of the vinylic double bond. The photophysical and photochemical properties have been also interpreted on the basis of quantum chemical calculations. All the examined compounds exhibit reduction processes at mild negative potentials that reveal their electron accepting character. We found that the photophysical, photochemical and electrochemical properties of such compounds are not only determined by the structure of the N-heterocyclic central moiety, but are also remarkably affected by the peripheral substituents linked to the quaternarized nitrogen atoms.

Keywords: Viologen; Electrochemistry; Luminescence; Electron transfer; Photoisomerization

1. Introduction

The 4,4′-bipyridinium dication (V^{2+}) (Chart 1) is a commonplace among electron accepting units [1]. Its derivatives are widely employed in a large variety of applications, such as electron-transfer relays [2], redox-active units in molecular and supramolecular systems [3], molecular machines [4], molecular electronics [5], electrochromic systems [6], and charge-transfer salts [1]. The prototypical species, 1,1′-dimethyl-4,4′-bipyridinium – also known as methylviologen or paraquat – was formerly used as a herbicide [7].

Several other compounds based on N-heterocycles, structurally related to 4,4′-bipyridinium, have been reported in the literature, and found to behave as efficient electron acceptors. Examples are the compounds of the 1,2-bis(4-pyridinium)ethylene (BPE^{2+}) [8,9] and 2,7-diazapyrenium (DAP^{2+}) [10,11] families (Chart 1). All these species share the nature of electron-poor π-systems, but possess quite distinct physicochemical properties. The peculiar feature of the first family resides in the possibility of undergoing photoinduced $E \rightarrow Z$ isomerization, whereas the most important property of the second family is that of exhibiting strong and structured fluorescence at room temperature, and structured fluorescence and phosphorescence in rigid matrix at 77 K.

Here, we report the results of photophysical, photochemical and electrochemical investigations in solution, and quantum chemical calculations, on three families of

* Corresponding authors. Tel.: +39 051 2099540; fax: +39 051 2099456.
E-mail addresses: alberto.credi@unibo.it (A. Credi), mariateresa.gandolfi@unibo.it (M.T. Gandolfi), margherita.venturi@unibo.it (M. Venturi).

0020-1693/$ - see front matter © 2006 Elsevier B.V. All rights reserved.
doi:10.1016/j.ica.2006.08.026

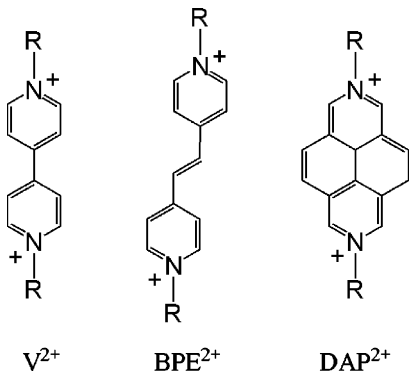

Chart 1. Generalized structural formulas of *N*,*N*-derivatives of 4,4′-bipyridinium (V^{2+}), *E*-1,2-bis(4-pyridinium)ethylene (BPE^{2+}), and 2,7-diazapyrenium (DAP^{2+}) cations.

compounds based on the 4,4′-bipyridinium, 1,2-bis(4-pyridinium)ethylene, and 2,7-diazapyrenium units, respectively (Chart 2). Within each family, we have examined compounds bearing either alkyl or aryl substituents on the quaternarized nitrogen atoms, showing that their spectroscopic and electrochemical properties are fine tuned by the nature of the substituents.

2. Experimental

2.1. Materials

All the compounds were available as hexafluorophosphate salts (unless otherwise noted) from previous investigations [8–11]. The acetonitrile (AN) and butyronitrile (BN) solvents, and all other chemicals were purchased from Merck, Romil or Aldrich, and used as received.

2.2. Absorption and luminescence spectra

The absorption spectra were recorded with Perkin–Elmer λ16 or λ40 spectrophotometers, while the luminescence spectra were obtained with a Perkin–Elmer LS50 spectrofluorimeter. All the spectra were obtained on air equilibrated AN (Merck Uvasol) solutions contained in quartz cells. The emission spectra in butyronitrile rigid matrix at 77 K were recorded on quartz tubes immersed in a quartz Dewar filled with liquid nitrogen. The luminescence quantum yields were determined by the optically dilute method using naphthalene or 9,10-diphenylanthracene in degassed cyclohexane, or quinine sulfate in 0.5 mol L^{-1} H_2SO_4, as standards [12]. The luminescence

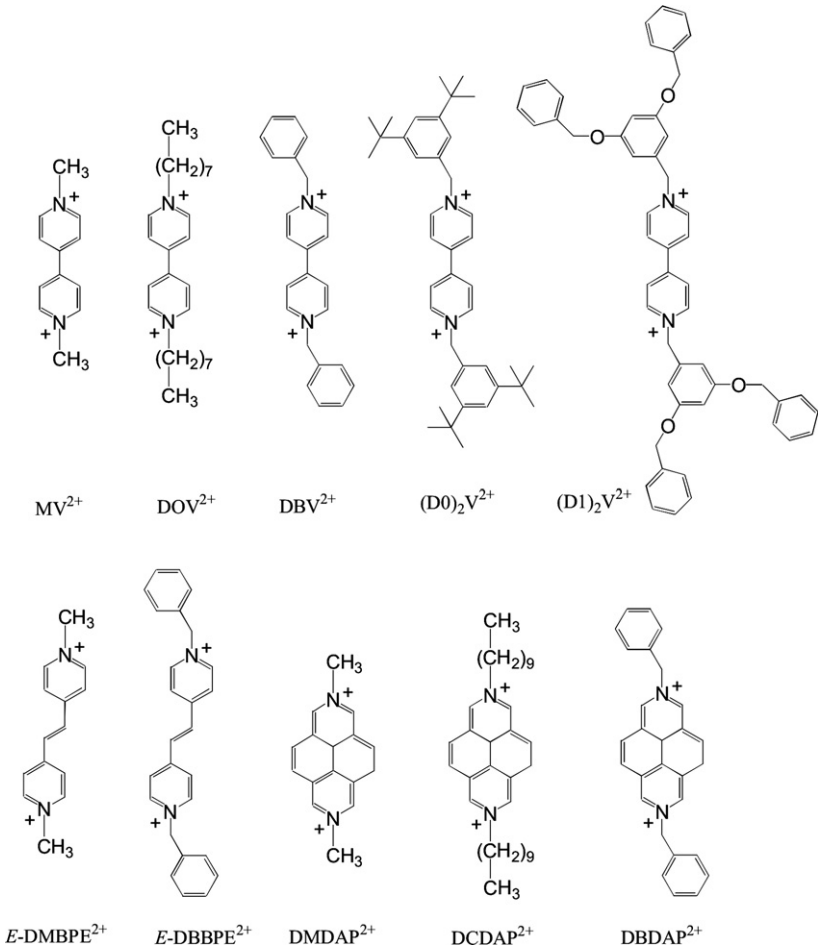

Chart 2. Structural formulas of the investigated compounds.

lifetimes were measured with a time-correlated single-photon counting apparatus (Edinburgh DS199); the excitation source was a deuterium-filled arc lamp. The experimental errors are wavelengths, ±1 nm; luminescence quantum yields, ±15%; and lifetimes, ±10%.

2.3. Photochemistry

Photochemical experiments were carried out in spectrofluorimetric cells on *E*-DMBPE^{2+} or *E*-DBBPE^{2+} 4.0×10^{-5} mol L^{-1} AN solutions at room temperature with a medium pressure mercury lamp (Hanau Q400, 150 W); the emission lines (313 nm for direct photochemistry, 365 and 436 nm for benzanthrone and biacetyl photosensitized reactions, respectively) were isolated by means of interference filters. The photosensitized experiments were performed on solutions degassed by four freeze–pump–thaw cycles and containing 2.0×10^{-5} mol L^{-1} *E*-DBBPE^{2+} and 6.0×10^{-2} mol L^{-1} biacetyl. In such experiments, the biacetyl phosphorescence was quenched with a rate constant of 1.5×10^{9} L mol^{-1} s^{-1}. Similar conditions were employed for the benzanthrone-sensitized experiments. The incident light intensity, measured by ferric oxalate actinometry [12], resulted to be of the order of 10^{-7} Nhν min^{-1} in the direct irradiation experiments, while in the photosensitized ones the intensity was reduced by means of a grey filter ($T = 1\%$). The photoreaction quantum yields were calculated [12] on the basis of the reactant disappearance, evaluated from the absorption changes; extrapolation to zero time was performed if necessary. Experimental error on the photoreaction quantum yields is ±20%.

2.4. Quantum chemical calculations

The energies and the oscillator strengths of the relevant electronic states as well as the energy of the low-lying triplet state closest to S_1 were calculated at the ZINDO/S level as implemented in the HYPERCHEM software [13]. The radiative (k_r) and total (k_t) deactivation rate constants were computed by means of the following relationships [14]:

$$k_r = k_r^{ref}\frac{f}{f_{ref}}\frac{\nu}{\nu_{ref}^2} \quad \text{and} \quad k_t = \frac{k_r}{\Phi_f},$$

where f, ν, and Φ_f represent, respectively, the calculated oscillator strength, the frequency of the lowest singlet state, and the fluorescence quantum yield; the index ref stands for a reference molecule, chosen as the π-isoelectronic 2,2′-bipyridine for MV^{2+} and DBV^{2+} [15], 1,2-bis(4-pyridine)ethylene for DMBPE^{2+} and DBBPE^{2+} [14], and pyrene for DMDAP^{2+} and DBDAP^{2+} [16].

2.5. Electrochemistry

Cyclic voltammetric (CV) and differential pulse voltammetric (DPV) experiments were carried out in an argon-purged AN (Romil Hi-Dry™) solution at room temperature with an Autolab 30 multipurpose instrument interfaced to a personal computer. The working electrode was a glassy carbon electrode (0.08 cm^2, Amel) and the counter electrode was a Pt spiral, separated from the bulk solution with a fine glass frit; a silver wire was employed as a quasi-reference electrode. The concentration of the compounds was in the range 5×10^{-4}–1×10^{-3} mol L^{-1} and tetraethylammonium hexafluorophosphate with 100 times higher concentration was added as supporting electrolyte. In all cases, ferrocene ($E_{1/2} = +0.395$ V versus SCE) was present as internal standard for the potential values. Cyclic voltammograms were obtained with sweep rates in the range 0.02–1.0 V s^{-1}; the IR compensation implemented within the Autolab 30 was used, and every effort was made throughout the experiments in order to minimize the resistance of the solution. In any instance, the full reversibility of the voltammetric wave of ferrocene was taken as an indicator of the absence of uncompensated resistance effects. The DPV experiments were performed with a scan rate of 20 or 4 mV s^{-1} (pulse height 75 and 10 mV, respectively) and a duration of 40 ms. The reversibility of the observed processes was established by using the criteria of: (i) separation of 60 mV between cathodic and anodic peaks, (ii) the close-to-unity ratio of the intensities of the cathodic and anodic currents, and (iii) the constancy of the peak potential on changing sweep rate in the cyclic voltammograms. For reversible processes, the same halfwave potential values were obtained from the DPV peaks and from an average of the cathodic and anodic CV peaks. The experimental error on the potential values was estimated to be ±10 mV. Spectroelectrochemical experiments were made in a spectrophotometric cell using a Pt grid as the working electrode; the counter electrode was a Pt wire, separated with a fine glass frit, and the reference electrode was an Amel Ag/AgCl. The absorption spectra of the reduced species were recorded with an Agilent Technologies 8543 diode array spectrophotometer.

3. Results and discussion

3.1. Absorption and luminescence properties

The experiments were carried out in AN solution at room temperature and in BN rigid matrix at 77 K. All the relevant data on the photophysical properties obtained in our laboratory are compiled in Tables 1–3, together with some data selected from the literature. Table 4 reports the calculated energies (ZINDO/S) of the emitting state, $E(S_1)$, its oscillator strength, f, the energy of the closest low-lying triplet state, $E(T_n)$, and the radiative, k_r, and total, k_t, deactivation rate constants.

3.1.1. Derivatives of 4,4′-bipyridinium

The absorption properties of the 1,1′-derivatives of 4,4′-bipyridinium ion have been extensively studied [1], while only a few, sometimes controversial data are available on their emission behavior [17,18]. The UV–Vis spectroscopic data on the investigated 4,4′-bipyridinium species are compiled in Table 1.

Table 1
Photophysical and electrochemical properties of 1,1′-derivatives of 4,4′-bipyridinium[a]

Compound	Absorption		Fluorescence at r.t.			Fluorescence at 77 K		Phosphorescence at 77 K		Electrochemistry	
	λ_{max} (nm)	ε (L mol^{-1} cm^{-1})	λ_{max} (nm)	τ (ns)	Φ	λ_{max} (nm)	τ (ns)	λ_{max} (nm)	τ (ms)	$E^{I}_{1/2}$ (V vs. SCE)	$E^{II}_{1/2}$ (V vs. SCE)
MV^{2+}	260[b]	20 000[b]	353[c]	0.9[c]	0.02[c]	330	7	418[d,e]	3600	−0.43[f]	−0.84[f]
DOV^{2+}	264	24 500	353	1	9×10^{-3}					−0.42[g]	−0.87[g]
DBV^{2+}	260	20 000								−0.35[h]	−0.78[h]
$(D0)_2V^{2+}$	259	29 000								−0.37	−0.79
$(D1)_2V^{2+}$	261	25 400								−0.34	−0.77

[a] Absorption and fluorescence spectra were performed at room temperature on air equilibrated AN solutions. Fluorescence and phosphorescence spectra at 77 K were recorded on BN rigid matrices. Electrochemical studies were performed in an argon-purged AN solution at room temperature; tetraethylammonium hexafluorophosphate as supporting electrolyte. For errors, see Section 2.
[b] From Ref. [19].
[c] In good agreement with the data from Ref. [17], where it is reported that the same results were obtained on a solution saturated with the chloride salt. The authors reported also a very weak emission in H_2O with $\lambda_{max} = 345$ nm, $\tau < 3$ ps.
[d] Structured band.
[e] Highest energy feature.
[f] From Ref. [31].
[g] Tosylate counterion.
[h] From Refs. [8,32].

Table 2
Photophysical, photochemical and electrochemical properties of *N*,*N*-derivatives of *E*-1,2-bis(4-pyridinium)ethylene[a]

Compound	Absorption		Fluorescence at r.t.			Fluorescence at 77 K		Phosphorescence at 77 K		Photochemistry		Electrochemistry	
	λ_{max} (nm)	ε (L mol^{-1} cm^{-1})	λ_{max} (nm)	τ (ns)	Φ	λ_{max} (nm)	τ (ns)	λ_{max} (nm)	τ (ms)	Φ_{dir}[b]	Φ_{sens}[b] (disaer)	$E^{I}_{1/2}$ (V vs. SCE)	$E^{II}_{1/2}$ (V vs. SCE)
E-$DMBPE^{2+}$	317	42 000	365	<1[c]	0.015	345[d,e]	1.2			0.35[f]		−0.50	−0.72
E-$DBBPE^{2+}$	324[g]	42 000[g]	372[g]	<1	6×10^{-4}[g]	352[d,e]	1.2			8×10^{-4}[g,h]	0.4[g,i]	−0.44[g]	−0.64[g]

[a] Absorption and fluorescence spectra and photochemical experiments with direct irradiation were performed at room temperature on air equilibrated AN solutions. The solutions used for photosensitized reactions were degassed by the freeze–pump–thaw method. Fluorescence and phosphorescence spectra at 77 K were recorded on BN rigid matrices. Electrochemical studies were performed in argon-purged AN solution at room temperature; tetraethylammonium hexafluorophosphate as supporting electrolyte. For errors, see Section 2.
[b] Quantum yield values extrapolated at $t = 0$.
[c] $\tau = 50$ ps reported in Ref. [27].
[d] Structured band.
[e] Highest energy feature.
[f] $E \rightarrow Z$ photoisomerization, from Ref. [26].
[g] From Ref. [8].
[h] The photoproduct is a cyclobutene derivative.
[i] $E \rightarrow Z$ photoisomerization using biacetyl as sensitizer.

Table 3
Photophysical and electrochemical properties of *N*,*N*-derivatives of 2,7-diazapyrenium[a]

Compound	Absorption		Fluorescence at r.t.			Fluorescence at 77 K		Phosphorescence at 77 K		Electrochemistry	
	λ_{max} (nm)	ε (L mol^{-1} cm^{-1})	λ_{max} (nm)	τ (ns)	Φ	λ_{max} (nm)	τ (ns)	λ_{max} (nm)	τ (ms)	$E^{I}_{1/2}$ (V vs. SCE)	$E^{II}_{1/2}$ (V vs. SCE)
$DMDAP^{2+}$[b]	335[c] 418[c]	33 000 15 000	423[c,d]	10.4	0.60	424[c,d]	10.7	586[c,d]	900	−0.46	[e]
$DCDAP^{2+}$	336[c] 418[c]	31 500 13 800	424[c,d]	9.5	0.5	428[c,d,f]	7.7[f]	585[c,d,f]	580[f]	−0.45	[e]
$DBDAP^{2+}$[b]	341[c] 421[c]	35 000 12 500	427[c,d]	4.3	0.28	427[c,d]	10.5	580[c,d]	750	−0.41	[e]

[a] Absorption and fluorescence spectra were performed at room temperature on air equilibrated AN solutions. Fluorescence and phosphorescence spectra at 77 K were recorded on BN rigid matrices. Electrochemical studies were performed in argon-purged AN solution at room temperature; tetraethylammonium hexafluorophosphate as supporting electrolyte. For errors, see Section 2.
[b] Ref. [11].
[c] Structured band.
[d] Highest energy feature.
[e] Irreversible process.
[f] In a 1:1 AN–BN rigid matrix.

Table 4
Calculated photophysical properties (ZINDO/S) for some of the investigated compounds

Compound	$E(S_1)$[a] (cm^{-1})	f[b]	$E(T_n)$[c] (cm^{-1})	$k_r \times 10^{-8}$[d] (s^{-1})	$k_t \times 10^{-10}$[e] (s^{-1})
MV^{2+}	34 600	0.01	28 410	0.02	0.1
DBV^{2+}	23 580	0.04	22 570	0.2	>45
E-$DMBPE^{2+}$	28 250	1.58	27 700	8.4	5.6
E-$DBBPE^{2+}$	24 510	0.18	24 210	1.3	22.7
$DMDAP^{2+}$	24 510	0.31	23 640	0.82	0.01
$DBDAP^{2+}$	24 450	0.28	24 390	0.74	0.03

[a] Energy of the lowest excited singlet state.
[b] S_1 oscillator strength.
[c] Energy of the low-lying triplet state closest to S_1.
[d] Radiative deactivation rate constant of the emitting state.
[e] Total deactivation rate constant of the emitting state.

The simplest compound of this family (Chart 2) is the 1,1′-dimethyl-4,4′-bipyridinium ion (MV^{2+}), whose absorption spectrum is reported in Fig. 1 [19], together with the spectra of the dibenzyl (DBV^{2+}) and dioctyl (DOV^{2+}) derivatives. A comparison of the absorption band shape is shown in Fig. 2. The absorption spectra exhibit in all cases an intense unstructured band centred at around 260 nm, attributed to a $\pi\pi^*$ (HOMO → LUMO)

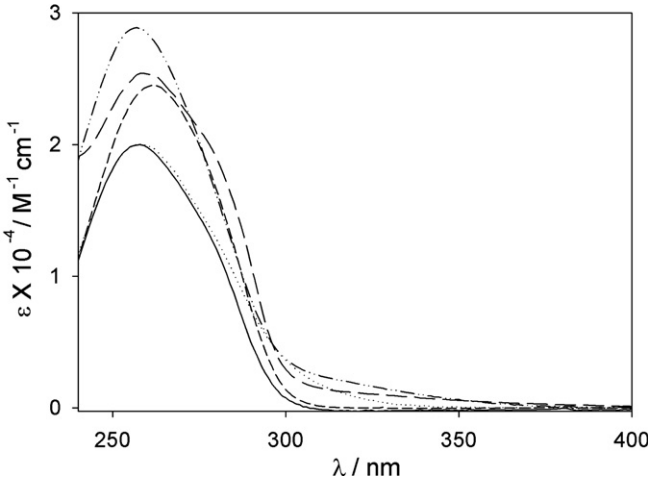

Fig. 1. Absorption spectra of MV^{2+} (——), DBV^{2+} (· · · · · ·), DOV^{2+} (– – – –), $(D0)_2V^{2+}$ (–·–·–·–·) and $(D1)_2V^{2+}$ (— — —) (AN, room temperature).

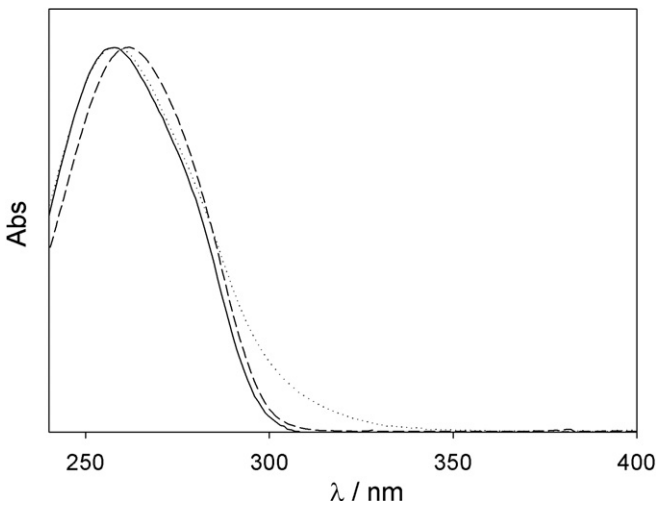

Fig. 2. Comparison of the absorption band shape of MV^{2+} (——), DBV^{2+} (· · · · · ·), and DOV^{2+} (– – – –) (AN, room temperature).

transition, calculated at 259 nm for MV^{2+}. For DOV^{2+}, the comparison shown in Fig. 2 evidences only a slight red shift of the maximum of the band, that can be assigned to a small perturbation caused by the presence of the two long aliphatic chains as substituents. For DBV^{2+}, an enlargement of the band toward longer wavelengths is present. In Fig. 1 the spectra of the di-*tert*-butylbenzyl, $(D0)_2V^{2+}$, and dimethylenoxybenzyl, $(D1)_2V^{2+}$, derivatives of the 4,4′-bipyridinium unit (Chart 2) are also reported. One can observe a modest increase in the molar absorption coefficients with respect to MV^{2+} and weak and long tails toward the visible region. In the case of DBV^{2+}, this second feature can be attributed to the presence of a couple of weak states ($\lambda = 293$ and 278 nm; $f \sim 0.01$) calculated below the first absorbing state. In addition, for $(D1)_2V^{2+}$ the presence of a shoulder around 275 nm is due to the dimethylenoxybenzyl substituents that absorb in this region.

As far as the emission properties are concerned, it has been often reported that MV^{2+} is not fluorescent in fluid solutions [18]. On the contrary, our results agree with those reported in Ref. [17], in which the authors have definitely stated, with detailed steady-state and time-resolved fluorimetric measurements, that MV^{2+} (as hexafluorophosphate salt) exhibits an appreciable radiative decay path from its lowest singlet excited state ($\pi\pi^*$ in nature). The fluorescence spectrum is shown in Fig. 3, together with that of DOV^{2+}. As one can see, the band shape is the same, although the emission quantum yield of DOV^{2+} is about half of that of MV^{2+} (see Table 1). This result can be likely attributed to the presence of the two alkyl chains, which can effectively contribute to the internal conversion deactivation process. The derivatives DBV^{2+}, $(D0)_2V^{2+}$, and $(D1)_2V^{2+}$ do not show any luminescence, because the lowest singlet excited state, calculated at 424 nm for DBV^{2+}(corresponding to 23 580 cm^{-1}, see Table 4), has a negligible oscillator strength. Contrary to what happens for MV^{2+}, the HOMO of DBV^{2+} is mainly localized on the benzyl substituents, whereas the LUMO is concentrated on the central bipyridinium ion: the promotion of electrons between S_0 and S_1 represents therefore a situation of intramolecular charge transfer, accompanied, in this case, by a very effective non-radiative deactivation channel (vide infra).

The deactivation of S_1 for MV^{2+} has been shown to be quite dependent on the solvent used [17]. In CH_3OH solution the main deactivation channel results in a photoreduction which is unequivocally detected by the presence of the monoreduced species, $MV^{+\cdot}$, following a 265 nm excitation in a pump–probe experiment [17]. On the other hand, in other solvents, like acetonitrile and water, different deactivation mechanisms seem to prevail: one of these can arise from the valence isomerization to a pre-fulvenic geometry of the pyridinium ion, in analogy to what was observed for pyridine in condensed phase [20]. In the case of DBV^{2+}, this process appears to be enhanced further, as shown by the very large value computed for k_t (Table 4) and the lack of phosphorescence at 77 K, although internal conversion to the ground state cannot be excluded owing to the relatively low energy of the S_1 state (23 580 cm^{-1}, Table 4).

3.1.2. Derivatives of 1,2-bis(4-pyridinium)ethylene

The 1,2-bis(4-pyridinium)ethylene dications are related to the class of stilbenes, and can exist in *E* and *Z* configurational isomers [21]. The absorption and luminescence data reported in this section are referred to the *E* isomers which are the thermodynamically stable forms. Information on the spectra of the *Z* isomers can be found in the next section dealing with photochemical behavior.

The UV–Vis spectroscopic data for the *N*,*N*-dimethyl and *N*,*N*-dibenzyl derivatives of *E*-1,2-bis(4-pyridinium)-ethylene in acetonitrile solution at room temperature and in butyronitrile glass at 77 K are compiled in Table 2. The absorption spectrum of *E*-$DBBPE^{2+}$ is similar to that of the dimethylated species *E*-$DMBPE^{2+}$, but slightly red-shifted (Fig. 4) and both show the typical fluorescence band

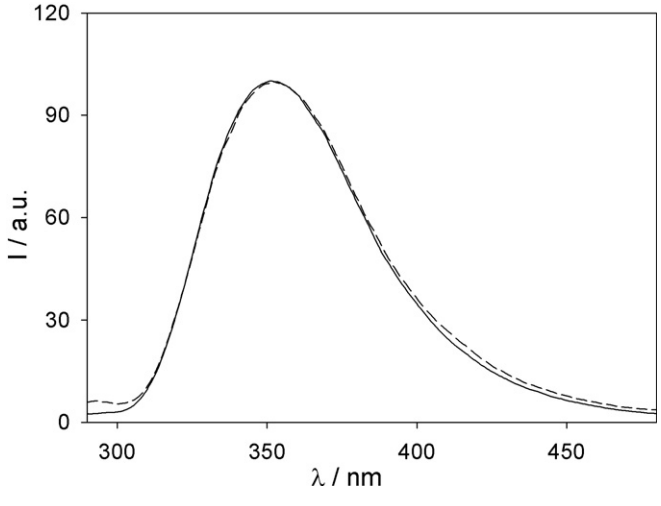

Fig. 3. Normalized fluorescence spectra of MV^{2+} (——) and DOV^{2+} (– – – –) (AN, room temperature, $\lambda_{exc} = 260$ nm).

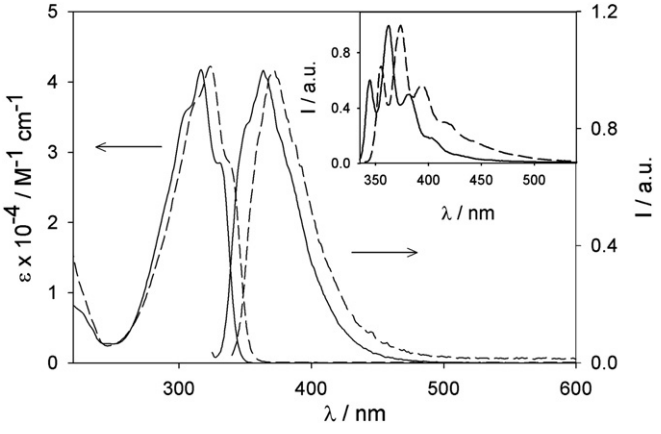

Fig. 4. Absorption and fluorescence spectra (AN, room temperature, $\lambda_{exc} = 320$ nm) of *E*-$DMBPE^{2+}$ (——) and *E*-$DBBPE^{2+}$ (– – – –). The inset shows the fluorescence spectra of *E*-$DMBPE^{2+}$ (——) and *E*-$DBBPE^{2+}$ (– – – –) in BN at 77 K ($\lambda_{exc} = 320$ nm). All the fluorescence spectra are normalized at the maximum intensity.

of the BPE^{2+} unit (Fig. 4) [22]; however, the luminescence quantum yield of *E*-$DBBPE^{2+}$ is only 4% of that of *E*-$DMBPE^{2+}$. This observation can be ascribed to the fact that the lowest singlet excited state in *E*-$DBBPE^{2+}$ has a charge-transfer nature, similarly to what discussed for DBV^{2+} (vide supra). This is not unexpected because the BPE^{2+} moiety is a good electron acceptor (vide infra) and the benzyl moiety can act as a weak reductant (the potential for the oxidation of toluene is +1.98 V versus SCE) [23]. Such a singlet state cannot be evidenced in the absorption spectrum, most likely because the corresponding electronic transition is characterized by a weak absorption coefficient (calculated $f = 0.18$) compared to that exhibited by the first absorbing system ($\varepsilon_{max} = 42000$ L mol^{-1} cm^{-1}, $f = 0.68$), but can effectively deactivate non-radiatively. In contrast to what happens for the unprotonated relative, 1,2-bis(4-pyridine)ethylene, where the $n\pi^*$ nature of the lowest singlet excited state coupled to a close lying $\pi\pi^*$ triplet induces an effective intersystem crossing [24], the triplet way of deactivation seems to be negligible for *E*-$DMBPE^{2+}$ and *E*-$DBBPE^{2+}$, as shown by the lack of phosphorescence at 77 K (Table 2). The relevant photophysical processes concerning the compounds $DMBPE^{2+}$ and $DBBPE^{2+}$ in their *E*-isomer are shown in Scheme 1.

3.1.3. Derivatives of 2,7-diazapyrenium

The UV–Vis spectroscopic data for the *N*,*N*-dimethyl, -didecanyl- and -dibenzyl derivatives of the 2,7-diazapyrenium unit in AN solution at room temperature and in BN glass at 77 K are compiled in Table 3.

The absorption spectra of all the investigated DAP^{2+} derivatives exhibit (Fig. 5) three intense and structured bands which can be assigned to transitions to the first, second, and third singlet $\pi\pi^*$ excited states, respectively. The absorption bands of $DBDAP^{2+}$ are slightly red shifted with respect to those of the parent alkyl-substituted species. The compounds of the DAP^{2+} family are most interesting for their luminescence properties [25]: they exhibit a very intense and structured fluorescence band with a lifetime in the ns time scale (Table 3); at 77 K, besides fluorescence, a structured phosphorescence band can also be seen (Fig. 5).

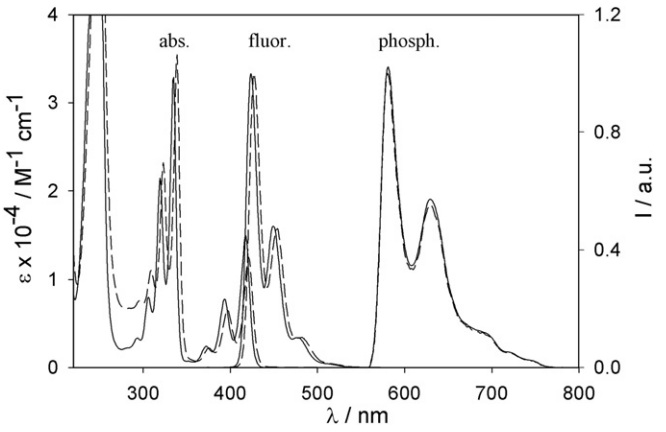

Fig. 5. Absorption and fluorescence spectra (AN, room temperature, $\lambda_{exc} = 390$ nm), and phosphorescence spectra (BN, 77 K, $\lambda_{exc} = 390$ nm) of $DMDAP^{2+}$ (——) and $DBDAP^{2+}$ (– – – –). All the luminescence spectra are normalized at the maximum intensity.

From an analysis of the radiative (k_r) and total (k_t) deactivation rate constants collected in Table 4, it can be noticed that for the compounds of the 4,4′-bipyridinium and BPE^{2+} families the main deactivation channel of the emitting state is due to non-radiative processes which depend essentially on the molecular structure of the compounds. This does not hold true for the DAP^{2+}-based species, for which k_r is comparable with k_t. The highly condensed and rigid DAP^{2+} moiety is strongly emissive because of the lack of torsion around single or double bonds – processes that represent major energy sinks for the bipyridinium- and BPE^{2+}-type species. In the case of the DAP^{2+}-based compounds a non-radiative channel may be identified with the population of a suitable T_n triplet state, followed by a $T_n \rightarrow T_1$ conversion and eventual phosphorescence. The difference in fluorescence quantum yield and lifetime values between the alkylated and benzylated compounds can be ascribed to a more efficient intersystem crossing to a T_n state in the case of $DBDAP^{2+}$. Indeed, for this compound the calculations show the presence of a triplet level nearly isoenergetic with S_1, and this can be taken as a hint for a very fast intersystem crossing process.

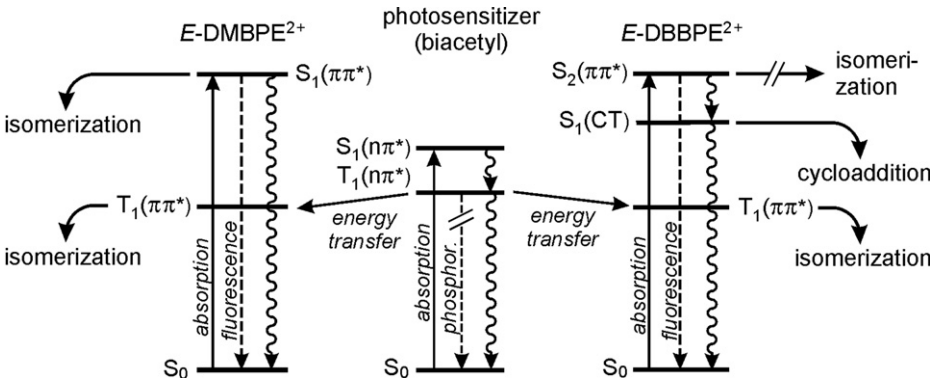

Scheme 1. Simplified energy-level diagram of the photophysical and photochemical processes that take place in *E*-$DMBPE^{2+}$ and *E*-$DBBPE^{2+}$. The wavy lines represent non-radiative processes.

3.2. Photochemical behavior

All the examined 4,4′-bipyridinium- and 2,7-diazapyrenium-type species are stable in solution upon irradiation with near UV light. On the contrary, the compounds containing the BPE^{2+} moiety exhibit interesting photochemical properties. The photoreactivity of 1,2-bis(4-pyridinium)ethylene derivatives was extensively investigated in the past [26–28], as well as that of the 1,2-bis(4-pyridyl)ethylene parent compound [29]. For *E*-$DMBPE^{2+}$ in AN solution, a $E \rightarrow Z$ photoisomerization reaction was observed upon both direct excitation in the $^1\pi\pi^*$ band [8,26] and triplet sensitization [8]. The absorption spectral changes associated with the photoisomerization are characterized by a clean isosbestic point at 286 nm. In our investigations, we found that *E*-$DBBPE^{2+}$ also undergoes a reaction in AN solution when irradiated in its $^1\pi\pi^*$ band at 313 nm. As shown in Fig. 6, the photoreaction causes a decrease in the intensity of such a band, and two isosbestic points (at 275 and 355 nm) are observed. After prolonged irradiation the isosbestic points are no longer maintained, and the $\pi\pi^*$ band disappears almost completely. The photoreaction takes place both in the presence and in the absence of oxygen, but it is slower in the latter case. The quantum yield for the disappearance of *E*-$DBBPE^{2+}$, measured from the change in the absorption spectrum at 340 nm (where the absorbance of the photoproduct can be neglected) is much smaller than that for the $E \rightarrow Z$ photoisomerization of *E*-$DMBPE^{2+}$ (Table 2). In fact, the characteristics of the spectral changes measured for $DBBPE^{2+}$ upon 313-nm irradiation rule out the possibility that the observed photoreaction is the $E \rightarrow Z$ isomerization about the vinylic double bond. From FABMS and ^{1}H NMR analyses we found [8] that the photoproduct is a cyclobutene derivative, thereby excluding the presence of the *Z* isomer in the reaction mixture.

To explore the possibility of obtaining the photoisomerization of *E*-$DBBPE^{2+}$, we performed photosensitization experiments by using biacetyl (energy of the lowest triplet excited state, $E_T = 19\,700\ cm^{-1}$ [12]) as a triplet sensitizer. In such experiments, a degassed AN solution containing *E*-$DBBPE^{2+}$ and biacetyl was irradiated with 436-nm light, absorbed exclusively by biacetyl. The absorption spectral changes observed (after subtraction of the biacetyl absorption, constant throughout the irradiation) are shown in Fig. 7 [8]. As one can see, the spectral changes are different from those observed upon direct excitation (Fig. 6), and an isosbestic point at 286 nm is present, as expected for the $E \rightarrow Z$ photoisomerization. The photoreaction quantum yield is 0.4; moreover, the absorption spectrum of the photoproduct is that expected for *Z*-$DBBPE^{2+}$ [27]. On prolonged irradiation the solution reaches a photostationary state, which corresponds to a $E \rightarrow Z$ conversion of 65%. When benzanthrone ($E_T = 16\,100\ cm^{-1}$ [12]) was used as a triplet sensitizer, the $E \rightarrow Z$ isomerization was again observed, with a lower quantum yield ($\Phi = 0.2$) and a photostationary state less displaced to the *Z* isomer (18%) [8]. On the basis of these results, the energy of the lowest triplet excited state of $DBBPE^{2+}$ can be estimated to be around $16\,000\ cm^{-1}$.

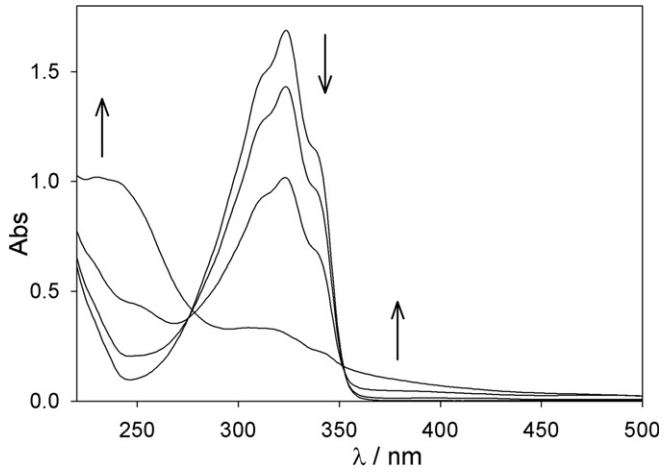

Fig. 6. Absorption changes for a 4.0×10^{-5} mol L^{-1} AN solution of *E*-$DBBPE^{2+}$ upon direct irradiation at 313 nm at room temperature.

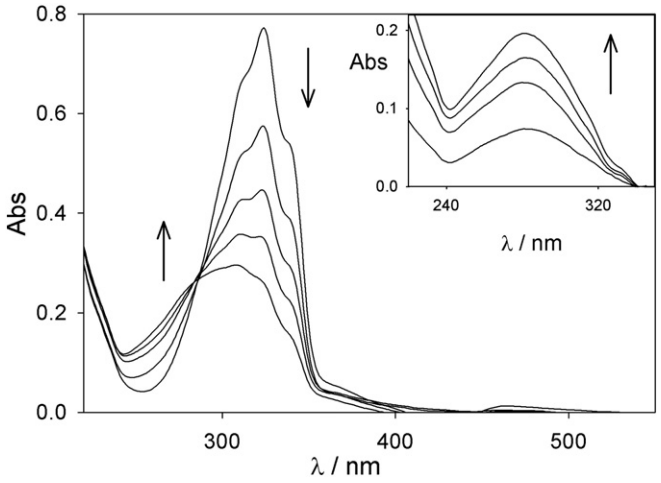

Fig. 7. Absorption changes observed for the photoreaction of *E*-$DBBPE^{2+}$ sensitized by biacetyl (degassed AN solution, room temperature, 2.0×10^{-5} mol L^{-1}, $\lambda_{irr} = 436$ nm); the absorbance of the sensitizer has been subtracted. The inset shows the spectral changes obtained when the absorbance of the unreacted *E*-$DBBPE^{2+}$ is also subtracted.

In summary, for *E*-$DMBPE^{2+}$ photoisomerization takes place by both direct ($^1\pi\pi^*$) and sensitized ($^3\pi\pi^*$) routes; furthermore, excitation to the $^1\pi\pi^*$ state causes a relatively strong fluorescence. Instead, for *E*-$DBBPE^{2+}$ irradiation on the $^1\pi\pi^*$ absorption band gives rise to a very weak fluorescence, and causes a photocycloaddition reaction rather than a photoisomerization (Scheme 1). These results can be again rationalized by considering the change in the nature of S_1 in going from the methyl to the benzyl substituted compound. The π-electron cloud in the S_1 state, owing to its CT character, is much more delocalized in *E*-$DBBPE^{2+}$ than it is in *E*-$DMBPE^{2+}$. This different electronic distribution not only causes a consistent decrease of the radiative rate constant in going from *E*-$DMBPE^{2+}$ to *E*-$DBBPE^{2+}$

(vide supra), but also influences the non-radiative pathways. Indeed, in *E*-DMBPE^{2+} a direct efficient photoisomerization occurs, while irradiation on the $^{1}\pi\pi^{*}$ absorption band of *E*-DBBPE^{2+} causes a cycloaddition reaction with a small quantum yield rather than isomerization (Table 2). In *E*-DBBPE^{2+} quite an efficient photoisomerization occurs via triplet sensitization. This indicates a different mechanism of $E \rightarrow Z$ photoisomerization, i.e., a direct process through the singlet manifold for *E*-DMBPE^{2+} and a sensitized one through the triplet manifold for *E*-DBBPE^{2+}, in analogy to what was observed for stilbene [30].

3.3. Electrochemical properties

The compounds dealt with in this paper (Chart 2) exhibit very similar electrochemical behavior which in several cases has been well established for a long time [1,3]. Independently on the substituents on the nitrogen atoms, in the potential window examined (from −1.8 to +1.8 V versus SCE) all the compounds show two consecutive reduction processes, and no oxidation process. However, the chemical nature of the substituents and the polarity of the solvent are expected to affect the values of the halfwave potentials at which the two reductions occur. Here we will discuss only the results obtained in acetonitrile solution.

3.3.1. Derivatives of 4,4′-bipyridinium

As already mentioned, 1,1′-dimethyl-4,4′-bipyridinium (MV^{2+}, Chart 2) is the simplest model for the bipyridinium-type dications. It exhibits two reversible and monoelectronic reduction processes at −0.43 and −0.84 V versus SCE [31] (Table 1, Fig. 8). The 1,1′-dioctyl derivative (DOV^{2+}, Chart 2) shows a practically identical behavior as far as reversibility, exchanged electrons, and halfwave potential values are concerned (Table 1). This result is not surprising by considering that the methyl and octyl groups are very similar alkyl substituents. In going to the 1,1′-dibenzyl derivative, DBV^{2+}, although two reversible and monoelectronic processes are again present, a positive shift of the halfwave potential values of both the reductions is observed (Table 1) [8,32]. This finding can be explained on the basis of two slightly different viewpoints that, however, lead to the same conclusion. The first interpretation is based upon the electron withdrawing character of the benzylic group, whereas the second one takes into account hyperconjugation effects [33]. They allow for the electronic communication between the bipyridinium and phenyl aromatic moieties via the methylene bridge, thereby increasing the charge delocalization, hence facilitating the electron uptake. The same considerations can be used to explain the behavior of $(D0)_2V^{2+}$ and $(D1)_2V^{2+}$ (Chart 2), which show a positive shift of the halfwave potential values similar to that observed for the dibenzyl derivative (Table 1).

It is also important to note that the monoreduced and doubly reduced species of most of the 1,1′-derivatives of 4,4′-bipyridinium are stable in carefully deoxygenated solution; in particular, the monoreduced species are intensely colored, owing to the presence of an unpaired electron acquired on reduction, and, depending on concentration, nature of the solvent, and temperature, can undergo dimerization [1]. As an example, Fig. 9 shows the absorption spectrum of the monoreduced species of DBV^{2+}, obtained in spectroelectrochemical experiments, whose features are similar to those of $MV^{+\cdot}$ [17].

3.3.2. Derivatives of 1,2-bis(4-pyridinium)ethylene

The electrochemical data reported below are referred to derivatives of the 1,2-bis(4-pyridinium)ethylene in the *E* isomeric form, which is stable under normal conditions.

The electrochemical behavior of the methyl and benzyl derivatives of *E*-1,2-bis(4-pyridinium)ethylene, characterized by two consecutive reversible, and monoelectronic

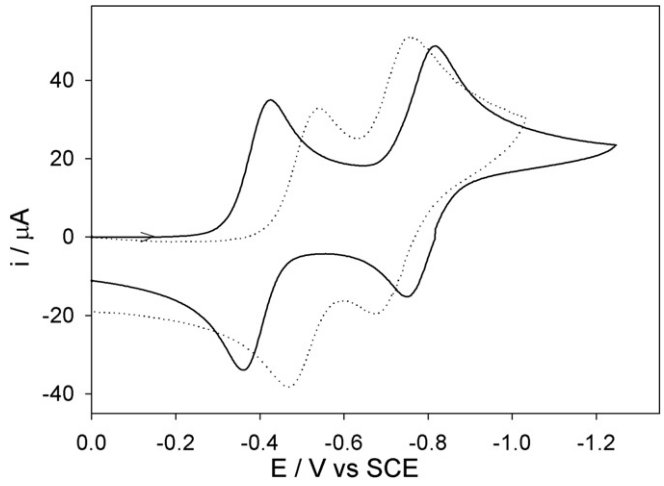

Fig. 8. Cyclic voltammetric patterns for the reduction of 1 mM MV^{2+} (——) and *E*-DMBPE^{2+} (·····). Conditions: argon-purged AN, room temperature, 200 mV s^{-1}, glassy carbon electrode; tetraethylammonium hexafluorophosphate as a supporting electrolyte.

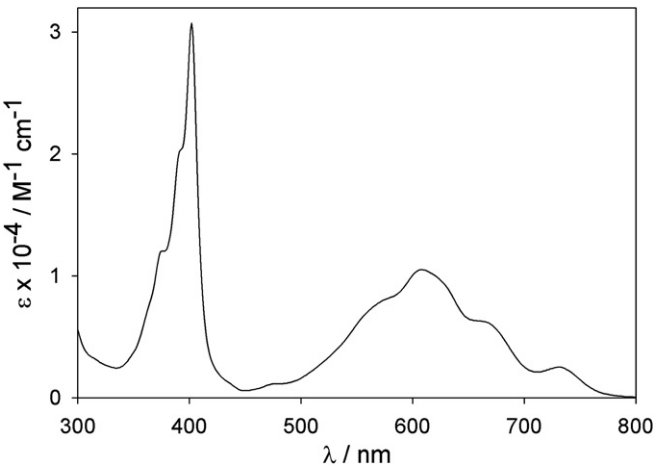

Fig. 9. Absorption spectrum of the monoreduced $DBV^{+\cdot}$ species (argon-purged AN, room temperature).

reduction processes, is very similar to that of the analogous 4,4′-bipyridinium cations (Table 2). It is, however, interesting to note that the first reduction takes place at potential values more negative, while the opposite occurs as far as the second reduction is concerned (Fig. 8). This finding can be understood by considering that in the *E*-1,2-bis(4-pyridinium)ethylene derivatives the two pyridinium rings, being separated by a double bond, are expected to be less electronically coupled than in the case of the 4,4′-bipyridinium analogues, in which the two pyridinium rings are directly linked. As a consequence, the first electron added to the *E*-1,2-bis(4-pyridinium)ethylene derivatives is less delocalized than in the 4,4′-bipyridinium ones, making the first reduction more difficult. For the same reason, the second electron added to the *E*-1,2-bis(4-pyridinium)ethylene derivatives is not much destabilized by the presence of the first electron, thereby making the second reduction easier than in the case of the 4,4′-bipyridinium analogues.

As for the 4,4′-bipyridinium family, the halfwave potential values of *E*-DBBPE^{2+}, are positively shifted in comparison to those obtained for *E*-DMBPE^{2+} (Table 2) [8]. This positive shift can be interpreted on the basis of the considerations made for the analogous 4,4′-bipyridinium derivative.

In the case of *E*-DBBPE^{2+}, the monoreduced species has also been obtained in spectroelectrochemical experiments. This species is stable in the dark and in carefully deoxygenated solutions, and displays a very characteristic absorption spectrum that confers a pink color to the solution (Fig. 10).

3.3.3. Derivatives of 2,7-diazapyrenium

The 2,7-diazapyrenium derivatives (Chart 2) are characterized by a large, flat and electron-poor surface [34a]. While their photophysical behavior is similar to that of pyrene, the electrochemical properties resemble, but are not as nice as those of the 4,4′-bipyridinium dications. They indeed show a first reduction process that is monoelectronic and reversible, like that exhibited by the 4,4′-bipyridinium analogues, and a second reduction process, which is irreversible and characterized by a low current intensity, most probably because of the chemical instability of the reduced species [25,34]. For this reason we consider only the halfwave potential values concerning the first reduction process. The data compiled in Table 3 show that the dimethyl, DMDAP^{2+} [11], and the didecanyl, DCDAP^{2+}, derivatives undergo the first reduction at a potential very similar to that of the corresponding 4,4′-bipyridinium derivatives. Moreover, in agreement with the results obtained for the two previously discussed families of compounds, and for the same reasons, in going to the dibenzyl derivative, DBDAP^{2+}, a shift of the first reduction potential toward less negative values is observed [11].

We have attempted to obtain the monoreduced form of the 2,7-diazapyrenium derivatives by using a variety of techniques (chemical reduction, electrolysis, radiation chemistry), but the results of these bulk reduction experiments could not be rationalized because they are highly dependent on the experimental conditions (solvent, light, time, etc.), confirming that the monoreduced forms of such derivatives are extremely reactive species.

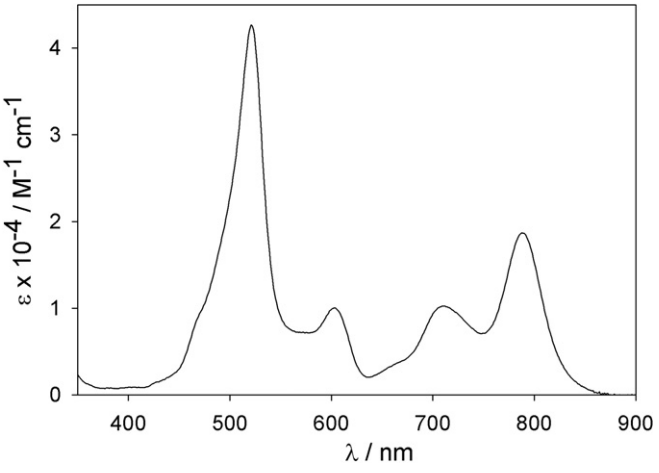

Fig. 10. Absorption spectrum of the monoreduced *E*-DBBPE$^{+\cdot}$ species (argon-purged AN, room temperature).

4. Conclusion

We have investigated the UV–Vis absorption and luminescence spectra, the photoreactivity, and the electrochemical properties of a series of aromatic electron acceptors based on the 4,4′-bipyridinium (V^{2+}), 1,2-bis(4-pyridinium)ethylene (BPE^{2+}), and 2,7-diazapyrenium (DAP^{2+}) dications (Chart 1). Quantum chemical calculations have also been performed in order to interpret the photophysical and photochemical behavior. While the 4,4′-bipyridinium derivatives are mostly interesting for their valuable electrochemical properties, the compounds of the BPE^{2+} family provide the possibility of studying the *E*–*Z* photoisomerization about the vinylic double bond, and the species based upon the DAP^{2+} moiety exhibit a strong luminescence, both fluorescence and phosphorescence. All the examined compounds undergo reduction processes at mild negative potentials that emphasize their electron accepting character. We found that the photophysical, photochemical and electrochemical properties of such compounds are not only determined by the structure of the central electron-accepting unit, but are also remarkably affected by the peripheral substituents linked to the quaternarized nitrogen atoms. Specifically, the different substitution with methyl or benzyl groups looks instrumental in modulating the photophysical behavior of these compounds, both by changing the energy and/or the nature of the lowest excited states, thereby possibly opening different channels for deactivation. Such effects are most evident in the compounds of the BPE^{2+} family, where N-benzyl substitution causes a fluorescence quenching and lack of $E \rightarrow Z$ photoisomerization in comparison with

the methyl derivative. In all cases, the presence of the benzyl substituents renders easier the electrochemical reduction of these compounds, owing to an increased delocalization of the added electron(s). These results can be helpful in the design of functional molecular and supramolecular systems and materials that make use of such electron-accepting moieties.

Acknowledgments

The financial support from Ministero dell'Istruzione, dell'Università e della Ricerca and Università di Bologna is gratefully acknowledged. We thank Giorgio Orlandi and Vincenzo Balzani for useful discussions.

References

[1] P.M.S. Monk, The Viologens – Physicochemical Properties, Synthesis and Application of the salts of 4,4′-Bipyridine, Wiley, Chichester, 1998.
[2] V. Balzani (Ed.), Electron Transfer in Chemistry, vols. 1–5, Wiley–VCH, Weinheim, 2001.
[3] A.E. Kaifer, M. Gómez-Kaifer, Supramolecular Electrochemistry, Wiley–VCH, Weinheim, 1999.
[4] V. Balzani, A. Credi, M. Venturi, Molecular Devices and Machines – A Journay into the Nanoworld, Wiley–VCH, Weinheim, 2003.
[5] Z. Li, B. Han, G. Meszaros, I. Pobelov, T. Wandlowski, A. Blaszczyk, M. Mayor, Faraday Discuss. 131 (2006) 121.
[6] A. Michaelis, H. Berneth, D. Haarer, S. Kostromine, R. Neigl, R. Schmidt, Adv. Mater. 13 (2001) 1825.
[7] A. Summers, The Bipyridinium Herbicides, Academic Press, New York, 1980.
[8] P.R. Ashton, R. Ballardini, V. Balzani, A. Credi, M.T. Gandolfi, S. Menzer, L. Pérez-García, L. Prodi, J.F. Stoddart, M. Venturi, A.J.P. White, D.J. Williams, J. Am. Chem. Soc. 117 (1995) 11171.
[9] R. Ballardini, V. Balzani, A. Credi, M.T. Gandolfi, L. Prodi, M. Venturi, L. Pérez-García, J.F. Stoddart, Gazz. Chim. Ital. 125 (1995) 353.
[10] (a) R. Ballardini, V. Balzani, A. Credi, M.T. Gandolfi, S.J. Langford, S. Menzer, L. Prodi, J.F. Stoddart, M. Venturi, D.J. Williams, Angew. Chem., Int. Ed. Engl. 35 (1996) 978;
(b) A. Credi, V. Balzani, S.J. Langford, J.F. Stoddart, J. Am. Chem. Soc. 119 (1997) 2679;
(c) P.R. Ashton, R. Ballardini, V. Balzani, E.C. Constable, A. Credi, O. Kocian, S.J. Langford, A.J. Preece, L. Prodi, E.R. Schofield, N. Spencer, J.F. Stoddart, S. Wenger, Chem. Eur. J. 4 (1998) 2413;
(d) A. Credi, M. Montalti, V. Balzani, S.J. Langford, F.M. Raymo, J.F. Stoddart, New J. Chem. 22 (1998) 1061.
[11] V. Balzani, A. Credi, S.J. Langford, A. Prodi, J.F. Stoddart, M. Venturi, Supramol. Chem. 13 (2001) 303.
[12] M. Montalti, A. Credi, L. Prodi, M.T. Gandolfi, Handbook of Photochemistry, third ed., CRC Press, Boca Raton, FL, 2006.
[13] HYPERCHEM ver. 6.02, Hypercube Inc., Gainesville, 2000.
[14] G. Orlandi, G. Poggi, G. Marconi, J. Chem. Soc., Faraday Trans. 2 76 (1980) 598.
[15] E. Castellucci, L. Angeloni, G. Marconi, E. Venuti, I. Baraldi, J. Phys. Chem. 94 (1990) 1740.
[16] J.B. Birks, Photophysics of Aromatic Molecules, Wiley–Interscience, London, 1970, p. 129.
[17] J. Peon, X. Tan, J.D. Hoerner, C. Xia, Y.F. Luk, B. Kohler, J. Phys. Chem. A 105 (2001) 5768.
[18] (a) A.W.-H. Mau, J.M. Overbeek, J.W. Loder, W.H.F. Sasse, J. Chem. Soc., Faraday Trans. 2 82 (1986) 869;
(b) V. Novakovic, M.Z. Hoffman, J. Am. Chem. Soc. 109 (1987) 2341;
(c) M. Alvaro, H. Garcia, S. Garcia, J.C. Scaiano, J. Phys. Chem. B 101 (1997) 3043.
[19] P.R. Ashton, R. Ballardini, V. Balzani, M. Belohradsky, M.T. Gandolfi, D. Philp, L. Prodi, F.M. Raymo, M.V. Reddington, N. Spencer, J.F. Stoddart, M. Venturi, D.J. Williams, J. Am. Chem. Soc. 118 (1996) 4931.
[20] M. Chachisvillis, A.H. Zewail, J. Phys. Chem. A 103 (1999) 7408.
[21] H. Dürr, H. Bouas-Laurent (Eds.), Photochromism: Molecules and Systems, Elsevier, Amsterdam, 2003.
[22] G. Favaro, G. Beggiato, Gazz. Chim. Ital. 100 (1970) 326.
[23] C.K. Mann, K.K. Barnes, Electrochemical Reactions in Non-aqueous Systems, Dekker, New York, 1970.
[24] G. Buntinx, R. Naskrecki, O. Poizat, J. Phys. Chem. 100 (1996) 19380.
[25] A.M. Brun, A. Harriman, J. Am. Chem. Soc. 113 (1991) 8153.
[26] T.W. Ebbesen, C.M. Previtali, T. Karatsu, T. Arai, K. Tokumaru, Chem. Phys. Lett. 119 (1985) 489.
[27] T.W. Ebbesen, K. Tokumaru, M. Sumitani, K. Yoshihara, J. Phys. Chem. 93 (1989) 5453.
[28] T.W. Ebbesen, R. Akaba, K. Tokumaru, M. Washio, S. Tagava, Y. Tabata, J. Am. Chem. Soc. 110 (1988) 2147.
[29] D.G. Whitten, M.T. McCall, J. Am. Chem. Soc. 91 (1969) 5097.
[30] (a) G. Orlandi, G. Marconi, Chem. Phys. 8 (1975) 458;
(b) G. Orlandi, G. Marconi, Il Nuovo Cimento 63B (1981) 332.
[31] P.L. Anelli, P.R. Ashton, R. Ballardini, V. Balzani, M. Delgado, M.T. Gandolfi, T.T. Goodnow, A.E. Kaifer, D. Philp, M. Pietraszkiewicz, L. Prodi, M.V. Reddington, A.M.Z. Slawin, N. Spencer, J.F. Stoddart, C. Vincent, D.J. Williams, J. Am. Chem. Soc. 114 (1992) 193.
[32] D.B. Amabilino, P.R. Ashton, V. Balzani, C.L. Brown, A. Credi, J.M.J. Fréchet, J.W. Leon, F.M. Raymo, N. Spencer, J.F. Stoddart, M. Venturi, J. Am. Chem. Soc. 118 (1996) 12012.
[33] F.A. Carey, R.J. Sundberg, Advanced Organic Chemistry, Kluwer Academic/Plenum Press, New York, 2000.
[34] (a) A.J. Blacker, J. Jazwinski, J.-M. Lehn, Helv. Chim. Acta 70 (1987) 1, and references therein;
(b) E.F. Lier, S. Hünig, H. Quast, Angew. Chem., Int. Ed. Engl. 7 (1968) 814.